Heliyon 10 (2024) e30751

Contents lists available at ScienceDirect

Heliyon

journal homepage: www.cell.com/heliyon

Research article

Weighted Mostar invariants of chemical compounds: An analysis of structural stability

Zahid Raza [a,*], Noor ul Huda [c], Farhana Yasmeen [b,c], Kashif Ali [c], Shehnaz Akhter [d], Yuqing Lin [e]

[a] Department of Mathematics, College of Sciences, University of Sharjah, United Arab Emirates
[b] Department of Mathematics, University of Okara, Okara, Pakistan
[c] Department of Mathematics, COMSATS University Islamabad, Lahore Campus, Pakistan
[d] School of Natural Sciences, National University of Sciences and Technology, Islamabad, Pakistan
[e] School of Information and Physical Sciences, The University of Newcastle, Australia

ARTICLE INFO

Keywords:
Weighted Mostar invariant
SIO_2 nanostructure
Poly-methyl methacrylate network $PMMA(s)$
Melem chains $MC(h)$ nanostructure

ABSTRACT

The concept of the weighted Mostar invariant is a mathematical tool used in chemical graph theory to study the stability of chemical compounds. Several recent studies have explored the weighted Mostar invariant of various chemical structures, including hydrocarbons, alcohols, and other organic compounds. One of the key advantages of the weighted Mostar invariant is that it can be easily computed for large and complex chemical structures, making it a valuable tool for studying the stability of a wide range of chemical compounds. This notion has been utilized to build novel approaches for forecasting chemical compound stability, such as machine learning algorithms. The focus of the paper is to demonstrate the weighted Mostar indices of three specific nanostructures: silicon dioxide (SIO_2, poly-methyl methacrylate network ($PMMA(s)$), and melem chains ($MC(h)$). The authors seek to provide the findings of their investigation of these nanostructures using the weighted Mostar invariant.

1. Introduction

A topological invariant or a connectivity invariant, also known as molecular invariant, is a mathematical expression that can be implemented on graphs that represent molecular structures. The invariant can be used to evaluate and further explore molecule's physicochemical characteristics. As a result, it is an effective method to ignore complicated and exorbitant laboratory experiments [16].

Topological descriptors have many applications, not only through toxicology, mathematical chemistry and drug discovery, but also in portraying diverse structural properties of networks [13]. The advancement of topological invariants is valuable in quantitative structure - activity and property relations [5,6,23].

The graphs discussed in this article are undirected, simple, and finite molecular graphs. Let $\mathsf{H} = (V_{\mathsf{H}}, E_{\mathsf{H}})$ be a graph having vertex set V_{H} and the edge set E_{H}, where $|V_{\mathsf{H}}|$ and $|E_{\mathsf{H}}|$ denote the order and size of H, respectively. The degree of $r \in V_{\mathsf{H}}$ is denoted as $deg_{\mathsf{H}}(r)$, and considered to be cardinality of edges directly linked with r.

* Corresponding author.
E-mail addresses: zraza@sharjah.ac.ae (Z. Raza), noorch071@gmail.com (N. ul Huda), farhanayasmeen@gmail.com (F. Yasmeen), akashifali@gmail.com (K. Ali), yuqing.lin@newcastle.edu.au (Y. Lin).

https://doi.org/10.1016/j.heliyon.2024.e30751
Received 18 January 2024; Received in revised form 17 April 2024; Accepted 3 May 2024

Available online 9 May 2024

It is reasonable to expect that the distance between two constituent elements (vertices) will influence their interaction. This motivates the research of a diverse group of distance-dependant topological descriptors. Another significant group is based on the basic characteristics of vertices, specifically their degrees [8,9,14]. There are also indices which aim to portray some relevant characteristics of entire graphs by evaluating contributions from every single vertex and/or edge. These are widely recognized as vertex-additive and bond-additive indices, respectively [26–28].

Edge contribution $\phi(e)$ can be expressed in the form of simple functions of quantitative characteristics of an edge's end vertices, which tells how similar the end vertices are. For example, $\phi(e) = |deg(r) - deg(z)|$ is an edge contribution that determines to what extent the end vertices vary in their degrees. The contributions over all edges compute how much G diverges from regularity. To further explore the concept of irregularity, see [1,10].

The peripheral edge in H is an edge having more vertices nearer to its one end vertex than to the other end-vertex. For a peripheral edge $rz \in E_{\mathsf{H}}$, denoted by $\mathsf{n}_z(rz|E_{\mathsf{H}})$ cardinality of vertices nearer to z than to r and presented by $\mathsf{n}_r(rz|E_{\mathsf{H}})$ cardinality of vertices nearer to r than to z. The Mostar index was introduced by Došlić et al. [11], it computes the edge contribution of $|\mathsf{n}_r(e|\mathsf{H}) - \mathsf{n}_z(e|\mathsf{H})|$ for an edge e. For a graph H, the Mostar invariant is:

$$Mo_{\upsilon}(\mathsf{H}) = \sum_{e=rz\in E_{\mathsf{H}}} |\mathsf{n}_r(e|\mathsf{H}) - \mathsf{n}_z(e|\mathsf{H})|.$$

Mostar invariant of benzenoid system was evaluated by Deng et al. [12] and they also compute the extremal Mostar invariant for unicyclic graphs and trees. After that, the results for the Mostar index of bicyclic graphs was computed in [24]. Tratnik [25] demonstrated that the Mostar index of a weighted graph can be extrapolated from Mostar index of a factor graph. Arockiaraj et al. [2] latterly presented edge and total Mostar invariants, which are extensions of the Mostar invariant:

$$Mo_e(\mathsf{H}) = \sum_{e=rz\in E_{\mathsf{H}}} |\mathsf{m}_r(e|\mathsf{H}) - \mathsf{m}_z(e|\mathsf{H})|,$$
$$Mo_t(\mathsf{H}) = \sum_{e=rz\in E_{\mathsf{H}}} |\mathsf{t}_r(e|\mathsf{H}) - \mathsf{t}_z(e|\mathsf{H})|,$$

where $\mathsf{m}_r(e|\mathsf{H})$ (or $\mathsf{m}_z(e|\mathsf{H})$) symbolize the total number of edges nearer to r (or z) than z (or r) and $\mathsf{t}_r(e|\mathsf{H})$ (or $\mathsf{t}_z(e|\mathsf{H})$) is the combined number of vertices and edges nearer to r (or z) than z (or r).

For an edge $e = rz \in E_{\mathsf{H}}$, there are two kinds of weights regarding degrees of end vertices.

$$W^*(e = rz) = deg_{\mathsf{H}}(r)deg_{\mathsf{H}}(z),\ W^+(e = rz) = deg_{\mathsf{H}}(r) + deg_{\mathsf{H}}(z).$$

Now, by using the above edge weights we can interpret the Mostar invariants for H as:

$$W^+Mo_{\upsilon}(\mathsf{H}) = \sum_{e=rz\in E_{\mathsf{H}}} W^+(e = rz)|\mathsf{n}_r(e|\mathsf{H}) - \mathsf{n}_z(e|\mathsf{H})|,$$
$$W^+Mo_e(\mathsf{H}) = \sum_{e=rz\in E_{\mathsf{H}}} W^+(e = rz)|\mathsf{m}_r(e|\mathsf{H}) - \mathsf{m}_z(e|\mathsf{H})|,$$
$$W^+Mo_t(\mathsf{H}) = \sum_{e=rz\in E_{\mathsf{H}}} W^+(e = rz)|\mathsf{t}_r(e|\mathsf{H}) - \mathsf{t}_z(e|\mathsf{H})|,$$
$$W^*Mo_{\upsilon}(\mathsf{H}) = \sum_{e=rz\in E_{\mathsf{H}}} W^*(e = rz)|\mathsf{n}_r(e|\mathsf{H}) - \mathsf{n}_z(e|\mathsf{H})|,$$
$$W^*Mo_e(\mathsf{H}) = \sum_{e=rz\in E_{\mathsf{H}}} W^*(e = rz)|\mathsf{m}_r(e|\mathsf{H}) - \mathsf{m}_z(e|\mathsf{H})|,$$
$$W^*Mo_t(\mathsf{H}) = \sum_{e=rz\in E_{\mathsf{H}}} W^*(e = rz)|\mathsf{t}_r(e|\mathsf{H}) - \mathsf{t}_z(e|\mathsf{H})|.$$

The research of computation and assessment of topological indices of molecular structures was driven with particular prominence in nanotechnology and mathematical chemistry. Readers are directed to references [3,4,7,15,17,18,30,29] for a more in-depth details on this subject.

The cut method was developed in [22] which partition of V_{H} of a graph $\mathsf{H} = (V_{\mathsf{H}}, E_{\mathsf{H}})$ into two subsets D and F, and compute the topological indices based on the cut $C = (\mathsf{D}, \mathsf{F})$. We used the cut method to compute the Mostar indices in this paper. Other topological indices of chemical graphs were also determined using this method, for example, the Wiener index [22].

2. Main results

Firstly, in section 2.1, with the help of the cut method, we evaluate the weighted plus Mostar invariants as well as the product Mostar invariants of melem chains $MC(h)$. While the section 2.2 presents weighted Mostar indices of poly-methyl methacrylate network $PMMA(s)$. Moreover, in section 2.3, we have developed the results for weighted plus and product Mostar invariants for the SIO_2 nanostructure.

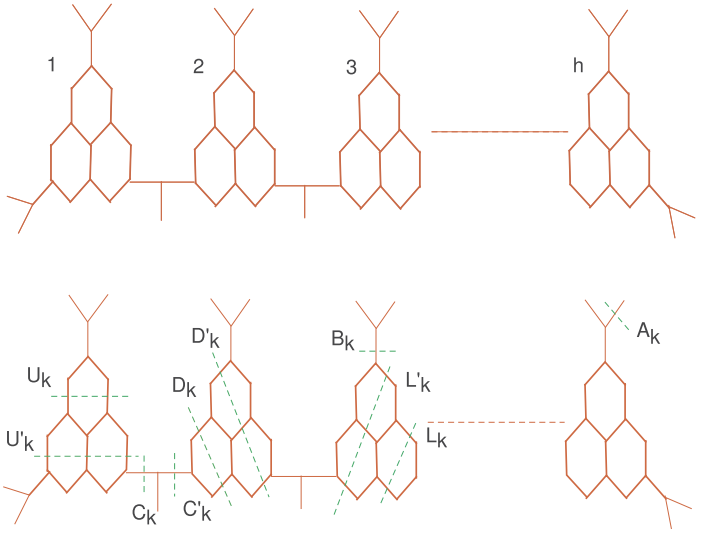

Fig. 1. Cuts of melem chain $MC(h)$.

Table 1
The values of $\mathfrak{n}_{MC(h)}(r)$, $\mathfrak{n}_{MC(h)}(s)$, $deg_{MC(h)}(r)$ and $deg_{MC(h)}(s)$ in A_k, B_k, D_k, L_k, U_k, D'_k, L'_k, U'_k, C_k and C'_k.

$rs \in E_{MC(h)}$	$\mathfrak{n}_{MC(h)}(r)$	$\mathfrak{n}_{MC(h)}(s)$	$deg_{MC(h)}(r)$	$deg_{MC(h)}(s)$	Frequency
A_k	$18h+3$	1	3	1	1
B_k	$18h+1$	3	3	3	1
$D_k = L_k = U_k$	$18k-12$	$18h+16-18k$	2	3	2
$D'_k = L'_k = U'_k$	$18k-7$	$18h+11-18k$	2	3	3
$C_k = C'_k$	$18k+1$	$18h+3-18k$	3	3	1

2.1. Weighted Mostar invariants of melem chains $MC(h)$ nanostructure

Using the single phase melem $C_6N_7(NH_2)_3$ (2,5,8-triamino-tri-s-triazine), melem chain is obtained which is a chain nanotube. Distinct thermal treatments of various less compressed C-N-H compounds (e.g., melamine $C_3N_3(NH_2)_3$, ammonium dicyanamide $NH_4[N(CN)_2]$, cyanamide H_2CN_2 or dicyandiamide $H_4C_2N_4$ correspondingly) at high temperatures of about 450^oC in sealed glass vials were performed in order to yield a single phase melem as crystalline powder [19]. The melem chain $MC(h)$, having $h \geq 1$, has order $|V_{MC(h)}| = 18n+4$ and size $|E_{MC(h)}| = 21h+3$ respectively.

All cuts of melem chain $MC(h)$ are shown in Fig. 1. Here we named horizontal cuts as U_k and U'_k, where $\{U_k : 1 \leq k \leq h\}$ and $\{U'_k : 1 \leq k \leq h\}$ respectively. Acute and Obtuse cuts of $MC(h)$ are represented by D_k, D'_k and L_k, L'_k where $1 \leq k \leq h$. Moreover the cuts on the pendent edges of $MC(h)$ are presented by A_k, having range $1 \leq k \leq 3(h+1)$, and they are on the boundaries of the molecular graph of $MC(h)$. The cuts on the edges which are adjacent to the pendent edges are presented as C_k, C'_k where $1 \leq k \leq h-1$ and B_k where $\{B_k : 1 \leq k \leq h+2\}$. It is clear that the cuts U_k, D_k and L_k are relatively symmetric to one another, where $1 \leq k \leq h$. Similarly, the cuts U'_k, D'_k and L'_k are also same to one another. All the pendent cuts A_k, where $1 \leq k \leq 3(h+1)$ are symmetric to one another, the same holds for all the B_k cuts, as well as all the cuts C_k and C'_k where $1 \leq k \leq h-1$.

All the values of $\mathfrak{n}_{MC(h)}(r)$, $\mathfrak{n}_{MC(h)}(s)$, $\mathfrak{m}_{MC(h)}(r)$ and $\mathfrak{m}_{MC(h)}(s)$ where $rs \in E_{MC(h)}$, with their corresponding degrees in A_k, B_k, D_k, L_k, U_k, D'_k, L'_k, U'_k, C_k and C'_k are described in the forthcoming Tables 1 and 2. Next, we compute weighted vertex, edge and total Mostar indices of $MC(h)$.

Theorem 2.1. *For melem chains $MC(h)$ nanostructure with $h \geq 1$, we have*

1. $W^+Mo_v(MC(h)) = -2700\lceil\frac{h}{2}\rceil^2 + 2700h\lceil\frac{h}{2}\rceil + 600\lceil\frac{h}{2}\rceil - 432\lfloor\frac{h}{2}\rfloor^2 + 432h\lfloor\frac{h}{2}\rfloor - 384\lfloor\frac{h}{2}\rfloor + 324h^2 + 120h + 24.$
2. $W^*Mo_v(MC(h)) = -3240\lceil\frac{h}{2}\rceil^2 + 3240h\lceil\frac{h}{2}\rceil + 720\lceil\frac{h}{2}\rceil - 648\lfloor\frac{h}{2}\rfloor^2 + 648h\lfloor\frac{h}{2}\rfloor - 576\lfloor\frac{h}{2}\rfloor + 324h^2 + 90h + 18.$

Proof. First, we have the following table. Using the values from Table 1, we acquire

$$
\begin{aligned}
W^{+}Mo_{v}(MC(h)) &= (2+3)3\sum_{k=1}^{h} 2|18k-12-(18h+16-18k)| + (2+3)3\sum_{k=1}^{h} 3|18k-7-(18h+11\\
&\quad -18k)| + (3+1)\sum_{k=1}^{3(h+1)} |18h+3-1| + (3+3)\sum_{k=1}^{h+2} |18h+1-3| + (3+3)2\sum_{k=1}^{h-1} |18k\\
&\quad +1-(18h+3-18k|.\\
&= 30\sum_{k=1}^{\lceil \frac{h}{2} \rceil} (18h+28) - 5\sum_{k=1}^{\lceil \frac{h}{2} \rceil} (216k) - 30\sum_{k=\lceil \frac{h}{2} \rceil}^{h} (18h+28) + 5\sum_{k=\lceil \frac{h}{2} \rceil}^{h} (216k)\\
&\quad +45\sum_{k=1}^{\lceil \frac{h}{2} \rceil} (18h+18) - 5\sum_{k=1}^{\lceil \frac{h}{2} \rceil} (324k) - 45\sum_{k=\lceil \frac{h}{2} \rceil}^{h} (18h+18) + 5\sum_{k=\lceil \frac{h}{2} \rceil}^{h} (324k)\\
&\quad +4\sum_{k=1}^{3(h+1)} (18h+2) + 6\sum_{k=1}^{h+2} (18h-2) + 12\sum_{k=1}^{\lfloor \frac{h}{2} \rfloor} (18h+2) - 6\sum_{k=1}^{\lfloor \frac{h}{2} \rfloor} (72k)\\
&\quad -12\sum_{k=\lfloor \frac{h}{2} \rfloor}^{h-1} (18h+2) + 6\sum_{k=\lfloor \frac{h}{2} \rfloor}^{h-1} (72k).\\
&= -2700\left\lceil \frac{h}{2} \right\rceil^{2} + 2700h\left\lceil \frac{h}{2} \right\rceil + 600\left\lceil \frac{h}{2} \right\rceil - 432\left\lfloor \frac{h}{2} \right\rfloor^{2} + 432h\left\lfloor \frac{h}{2} \right\rfloor - 384\left\lfloor \frac{h}{2} \right\rfloor\\
&\quad +324h^{2} + 120h + 24.
\end{aligned}
$$

$$
\begin{aligned}
W^{*}Mo_{v}(MC(h)) &= (2\times 3)3\sum_{k=1}^{h} 2|18k-12-(18h+16-18k)| + (2\times 3)3\sum_{k=1}^{h} 3|18k-7-(18h+11\\
&\quad -18k)| + (3\times 1)\sum_{k=1}^{3(h+1)} |18h+3-1| + (3\times 3)\sum_{k=1}^{h+2} |18+1-3| + (3\times 3)2\sum_{k=1}^{h-1} |18k\\
&\quad +1-(18h+3-18k)|.\\
&= 36\sum_{k=1}^{\lceil \frac{h}{2} \rceil} (18h+28) - 6\sum_{k=1}^{\lceil \frac{h}{2} \rceil} (216k) - 36\sum_{k=\lceil \frac{h}{2} \rceil}^{h} (18h+28) + 6\sum_{k=\lceil \frac{h}{2} \rceil}^{h} (216k)\\
&\quad +54\sum_{k=1}^{\lceil \frac{h}{2} \rceil} (18h+18) - 6\sum_{k=1}^{\lceil \frac{h}{2} \rceil} (324k) - 54\sum_{k=\lceil \frac{h}{2} \rceil}^{h} (18h+18) + 6\sum_{k=\lceil \frac{h}{2} \rceil}^{h} (324k)\\
&\quad +3\sum_{k=1}^{3(h+1)} (18h+2) + 9\sum_{k=1}^{h+2} (18h-2) + 18\sum_{k=1}^{\lfloor \frac{h}{2} \rfloor} (18h+2) - 9\sum_{k=1}^{\lfloor \frac{h}{2} \rfloor} (72k)\\
&\quad -18\sum_{k=\lfloor \frac{h}{2} \rfloor}^{h-1} (18h+2) + 9\sum_{k=\lfloor \frac{h}{2} \rfloor}^{h-1} (72k).\\
W^{*}Mo_{v}(MC(h)) &= -3240\left\lceil \frac{h}{2} \right\rceil^{2} + 3240h\left\lceil \frac{h}{2} \right\rceil + 720\left\lceil \frac{h}{2} \right\rceil - 648\left\lfloor \frac{h}{2} \right\rfloor^{2} + 648h\left\lfloor \frac{h}{2} \right\rfloor\\
&\quad -576\left\lfloor \frac{h}{2} \right\rfloor + 324h^{2} + 90h + 18. \quad \square
\end{aligned}
$$

Theorem 2.2. *For melem chains $MC(h)$, $h \geq 1$, nanostructure, we have*

1. $W^{+}Mo_{e}(MC(h)) = -3150\lceil \frac{h}{2} \rceil^{2} + 3150h\lceil \frac{h}{2} \rceil + 630\lceil \frac{h}{2} \rceil - 480\lfloor \frac{h}{2} \rfloor^{2} + 504h\lfloor \frac{h}{2} \rfloor - 480\lfloor \frac{h}{2} \rfloor + 366h^{2} + 213h.$
2. $W^{*}Mo_{e}(MC(h)) = -3780\lceil \frac{h}{2} \rceil^{2} + 3780h\lceil \frac{h}{2} \rceil + 756\lceil \frac{h}{2} \rceil - 720\lfloor \frac{h}{2} \rfloor^{2} + 756h\lfloor \frac{h}{2} \rfloor - 720\lfloor \frac{h}{2} \rfloor + 360h^{2} + 207h - 18.$

Proof. First, we have the following table.

Using the values of Table 2, we derive

$$
W^{+}Mo_{e}(MC(h)) = (2+3)3\sum_{k=1}^{h} 2|21k-16-(21h+17-21k)| + (2+3)3\sum_{k=1}^{h} 3|21k-10-(21h+10
$$

Table 2
The values of $\mathsf{m}_{MC(h)}(r)$, $\mathsf{m}_{MC(h)}(s)$, $deg_{MC(h)}(r)$ and $deg_{MC(h)}(s)$ in A_k, B_k, D_k, L_k, U_k, D'_k, L'_k, U'_k, C_k and C'_k.

$rs \in E_{MC(h)}$	$\mathsf{m}_{MC(h)}(r)$	$\mathsf{m}_{MC(h)}(s)$	$deg_{MC(h)}(r)$	$deg_{MC(h)}(s)$	Frequency
A_k	$21h+2$	0	3	1	1
B_k	$21h$	2	3	3	1
$D_k = L_k = U_k$	$21k-16$	$21h+17-21k$	2	3	2
$D'_k = L'_k = U'_k$	$21k-10$	$21h+10-21k$	2	3	3
$C_k = C'_k$	$20k+1$	$21h+1-20k$	3	3	1

$$-21k)| + (3+1)\sum_{k=1}^{3(h+1)} |21h+2-0| + (3+3)\sum_{k=1}^{h+2} |21h-2| + (3+3)2\sum_{k=1}^{h-1} |20k+1 -(21h+1-20k)|$$

$$= 30\sum_{k=1}^{\lceil \frac{h}{2} \rceil} (21h+33) - 5\sum_{k=1}^{\lceil \frac{h}{2} \rceil} (252k) - 30\sum_{k=\lceil \frac{h}{2} \rceil}^{h} (21h+33) + 5\sum_{k=\lceil \frac{h}{2} \rceil}^{h} (252k) + 45\sum_{k=1}^{\lceil \frac{h}{2} \rceil} (21h + 20) - 5\sum_{k=1}^{\lceil \frac{h}{2} \rceil} (378k) - 45\sum_{k=\lceil \frac{h}{2} \rceil}^{h} (21h+20) + 5\sum_{k=\lceil \frac{h}{2} \rceil}^{h} (378k) + 4\sum_{k=1}^{3(h+1)} (21h+2) + 6\sum_{k=1}^{h+2} (21h-2) + 12\sum_{k=1}^{\lfloor \frac{h}{2} \rfloor} (21h) - 6\sum_{k=1}^{\lfloor \frac{h}{2} \rfloor} (80k) - 12\sum_{k=\lfloor \frac{h}{2} \rfloor}^{h-1} (21h) + 6\sum_{k=\lfloor \frac{h}{2} \rfloor}^{h-1} (80k)$$

$$W^+Mo_e(MC(h)) = -3150\left\lceil \frac{h}{2} \right\rceil^2 + 3150h\left\lceil \frac{h}{2} \right\rceil + 630\left\lceil \frac{h}{2} \right\rceil - 480\left\lfloor \frac{h}{2} \right\rfloor^2 + 504h\left\lfloor \frac{h}{2} \right\rfloor - 480\left\lfloor \frac{h}{2} \right\rfloor + 366h^2 + 213h.$$

$$W^*Mo_e(MC(h)) = (2\times 3)3\sum_{k=1}^{h} 2|21k-16-(21h+17-21k)| + (2\times 3)3\sum_{k=1}^{h} 3|21k-10-(21h+10 -21k)| + (3\times 1)\sum_{k=1}^{3(h+1)} |21h+2-0| + (3\times 3)\sum_{k=1}^{h+2} |21h-2| + (3\times 3)2\sum_{k=1}^{h-1} |20k+1 -(21h+1-20k)|.$$

$$= 36\sum_{k=1}^{\lceil \frac{h}{2} \rceil} (21h+33) - 6\sum_{k=1}^{\lceil \frac{h}{2} \rceil} (252k) - 36\sum_{k=\lceil \frac{h}{2} \rceil}^{h} (21h+33) + 6\sum_{k=\lceil \frac{h}{2} \rceil}^{h} (252k) + 54\sum_{k=1}^{\lceil \frac{h}{2} \rceil} (21h + 20) - 6\sum_{k=1}^{\lceil \frac{h}{2} \rceil} (378k) - 54\sum_{k=\lceil \frac{h}{2} \rceil}^{h} (21h+20) + 6\sum_{k=\lceil \frac{h}{2} \rceil}^{h} (378k) + 3\sum_{k=1}^{3(h+1)} (21h+2) + 9\sum_{k=1}^{h+2} (21h-2) + 18\sum_{k=1}^{\lfloor \frac{h}{2} \rfloor} (21h) - 9\sum_{k=1}^{\lfloor \frac{h}{2} \rfloor} (80k) - 18\sum_{k=\lfloor \frac{h}{2} \rfloor}^{h-1} (21h) + 9\sum_{k=\lfloor \frac{h}{2} \rfloor}^{h-1} (80k).$$

$$= -3780\left\lceil \frac{h}{2} \right\rceil^2 + 3780h\left\lceil \frac{h}{2} \right\rceil + 756\left\lceil \frac{h}{2} \right\rceil - 720\left\lfloor \frac{h}{2} \right\rfloor^2 + 756h\left\lfloor \frac{h}{2} \right\rfloor - 720\left\lfloor \frac{h}{2} \right\rfloor + 360h^2 + 207h - 18. \quad \square$$

Corollary 2.1. *For the melem chains $MC(h)$ nanostructure with $h \geq 1$, we have*

1. $W^+Mo_t(MC(h)) = -5850\lceil \frac{h}{2} \rceil^2 + 5850h\lceil \frac{h}{2} \rceil + 1230\lceil \frac{h}{2} \rceil - 912\lfloor \frac{h}{2} \rfloor^2 + 936h\lfloor \frac{h}{2} \rfloor - 864\lfloor \frac{h}{2} \rfloor + 690h^2 + 333h + 24.$
2. $W^*Mo_t(MC(h)) = -7020\lceil \frac{h}{2} \rceil^2 + 7020h\lceil \frac{h}{2} \rceil + 1476\lceil \frac{h}{2} \rceil - 1368\lfloor \frac{h}{2} \rfloor^2 + 1404h\lfloor \frac{h}{2} \rfloor - 1296\lfloor \frac{h}{2} \rfloor + 684h^2 + 297h.$

2.2. Weighted Mostar indices of poly-methyl methacrylate network $PMMA(s)$

Poly-methyl methacrylate, also recognized as acrylic glass, is a synthetic polymer that is commonly used as a substitute for glass in products such as skylights, aircraft canopies, instrument panels, and medical technologies [20]. $PMMA(s)$ was introduced as the first substitute for vulcanite as a raw material for denture by Walter Wright (1937), and it quickly grew into the most widely used fabrication for denture bases [21].

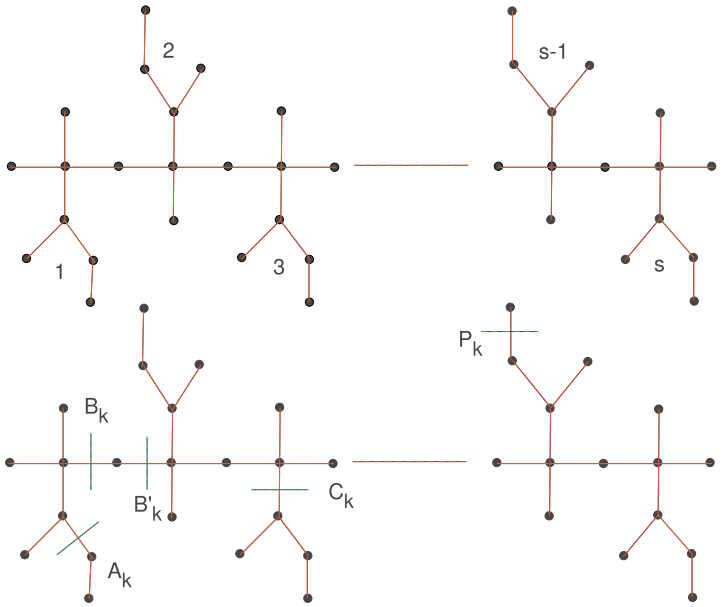

Fig. 2. Cuts of poly-methyl methacrylate network $PMMA(s)$.

Table 3
The values of $n_{PMMA(s)}(w)$ and $n_{PMMA(s)}(z)$ with their respective degrees in P_k, A_k, B_k, B'_k and C_k.

$wz \in E_{PMMA(s)}$	$n_{PMMA(s)}(w)$	$n_{PMMA(s)}(z)$	$deg_{PMMA(s)}(w)$	$deg_{PMMA(s)}(z)$	Frequency
P_k	$7s$	1	4	1	1
A_k	$7s-1$	2	2	3	1
$B_k = B'_k$	$7s+1-7k$	$7k$	4	2	1
C_k	$7s-3$	4	3	4	1

Denote by $PMMA(s)$ the s-dimensional hydrogen depleted - molecular structure of $PMMA$ as shown in Fig. 2, where s indicates the number of monomers in the polymer chain. The structure of $PMMA(s)$ has order $|V(PMMA(s))| = 7s+1$ and size $|E(PMMA(s))| = 7s$. The cuts of poly-methyl methacrylate network $PMMA(s)$ are shown in Fig. 2.

The cuts on the pendent edges of $PMMA(s)$ are denoted by P_k, where $1 \le k \le 3s+2$, and they sit on the boundaries of hydrogen depleted - molecular graph of $PMMA(s)$. The cuts on the joint edges to the pendent edges are named as A_k where $1 \le k \le s$. In the cuts other than these two cuts, the horizontal one is denoted by C_k where $\{C_k : 1 \le k \le s\}$ whereas the vertical ones are presented by B_k and B'_k where $1 \le k \le s-1$. In the following Tables 3 and 4, we give the values of $n_{PMMA(s)}(w)$ and $n_{PMMA(s)}(z)$ with their respective degrees in P_k, A_k, B_k, B'_k and C_k.

Here, we compute the weighted Mostar invariant of poly-methyl methacrylate network $PMMA(s)$.

Theorem 2.3. *For the poly-methyl methacrylate network $PMMA(s)$ with $s \ge 1$, we have*

1. $W^+Mo_v(PMMA(s)) = -168\lfloor\frac{s}{2}\rfloor^2 + 168s\lfloor\frac{s}{2}\rfloor - 144\lfloor\frac{s}{2}\rfloor + 189s^2 - 21s + 2.$
2. $W^*Mo_v(PMMA(s)) = -224\lfloor\frac{s}{2}\rfloor^2 + 224s\lfloor\frac{s}{2}\rfloor - 192\lfloor\frac{s}{2}\rfloor + 210s^2 - 74s + 8.$

Proof. Firstly, we have the following results

Using Table 3, we have the following.

$$W^+Mo_v(PMMA(s)) = (4+1)\sum_{k=1}^{3s+2}|7s-1| + (2+3)\sum_{k=1}^{s}|7s-1-2| + (3+4)\sum_{k=1}^{s}|7s-3-4|$$
$$+(4+2)\sum_{k=1}^{s-1}|7s+1-7k-(7k)|$$
$$= 5(3s+2)(7s-1) + 5s(7s-3) + 7s(7s-7) + 12(7s+1)\left\lfloor\frac{s}{2}\right\rfloor - (6)(14)\left(\left\lfloor\frac{s}{2}\right\rfloor^2 + \left\lfloor\frac{s}{2}\right\rfloor\right) - 12(7s+1)\left(s-1-\left\lfloor\frac{s}{2}\right\rfloor\right) + (6)(14)\left(s-1-\left\lfloor\frac{s}{2}\right\rfloor\right)\left(\left\lfloor\frac{s}{2}\right\rfloor + s\right)$$

Table 4
The values of $\mathsf{m}_{PMMA(s)}(w)$ and $\mathsf{m}_{PMMA(s)}(z)$ with their respective degrees in P_k, A_k, B_k, B'_k and C_k.

$wz \in E_{PMMA(s)}$	$m_{PMMA(s)}(w)$	$m_{PMMA(s)}(z)$	$deg_{PMMA(s)}(w)$	$deg_{PMMA(s)}(z)$	Frequency
P_k	$7s-1$	0	4	1	1
A_k	$7s-2$	1	2	3	1
$B_k = B'_k$	$7s-7k$	$7k-1$	4	2	1
C_k	$7s-4$	3	3	4	1

$$= -168\left\lfloor\frac{s}{2}\right\rfloor^2 + 168s\left\lfloor\frac{s}{2}\right\rfloor - 144\left\lfloor\frac{s}{2}\right\rfloor + 189s^2 - 21s + 2.$$

$$W^*Mo_v(PMMA(s)) = (4\times1)\sum_{k=1}^{3s+2}|7s-1| + (2\times3)\sum_{k=1}^{s}|7s-1-2| + (3\times4)\sum_{k=1}^{s}|7s-3-4|$$
$$+(4\times2)\sum_{k=1}^{s-1}|7s+1-7k-(7k)|$$
$$= 4(3s+2)(7s-1) + 6s(7s-3) + 12s(7s-7) + 16(7s+1)\left\lfloor\frac{s}{2}\right\rfloor - 112\left(\left\lfloor\frac{s}{2}\right\rfloor^2 + \left\lfloor\frac{s}{2}\right\rfloor\right) - 16(7s+1)\left(s-1-\left\lfloor\frac{s}{2}\right\rfloor\right) + 112\left(s-1-\left\lfloor\frac{s}{2}\right\rfloor\right)\left(\left\lfloor\frac{s}{2}\right\rfloor + s\right)$$
$$= -224\left\lfloor\frac{s}{2}\right\rfloor^2 + 224s\left\lfloor\frac{s}{2}\right\rfloor - 192\left\lfloor\frac{s}{2}\right\rfloor + 210s^2 - 74s + 8. \quad \square$$

Theorem 2.4. *For the poly-methyl methacrylate network $PMMA(s)$ with $s \geq 1$, we have*

1. $W^+Mo_e(PMMA(s)) = -168\lfloor\frac{s}{2}\rfloor^2 + 168s\lfloor\frac{s}{2}\rfloor - 144\lfloor\frac{s}{2}\rfloor + 189s^2 - 21s + 2.$
2. $W^*Mo_e(PMMA(s)) = -224\lfloor\frac{s}{2}\rfloor^2 + 224s\lfloor\frac{s}{2}\rfloor - 192\lfloor\frac{s}{2}\rfloor + 210s^2 - 74s + 8.$

Proof. Similar to the last proof, we have the following.

Using the values of $\mathsf{m}_{PMMA(s)}(w)$ and $\mathsf{m}_{PMMA(s)}(z)$ with their related degrees from Table 4, we acquire

$$W^+Mo_e(PMMA(s)) = (4+1)\sum_{k=1}^{3s+2}|7s-1-0| + (2+3)\sum_{k=1}^{s}|7s-2-1| + (3+4)\sum_{k=1}^{s}|7s-4-3|$$
$$+(4+2)\sum_{k=1}^{s-1}|7s-7k-(7k-1)|$$
$$= 5(3s+2)(7s-1) + 5s(7s-3) + 7s(7s-7) + 12(7s+1)\left\lfloor\frac{s}{2}\right\rfloor - (6)(14)\left(\left\lfloor\frac{s}{2}\right\rfloor^2 + \left\lfloor\frac{s}{2}\right\rfloor\right) - 12(7s+1)\left(s-1-\left\lfloor\frac{s}{2}\right\rfloor\right) + (6)(14)\left(s-1-\left\lfloor\frac{s}{2}\right\rfloor\right)\left(\left\lfloor\frac{s}{2}\right\rfloor + s\right)$$
$$= -168\left\lfloor\frac{s}{2}\right\rfloor^2 + 168s\left\lfloor\frac{s}{2}\right\rfloor - 144\left\lfloor\frac{s}{2}\right\rfloor + 189s^2 - 21s + 2.$$

$$W^*Mo_e(PMMA(s)) = (4\times1)\sum_{k=1}^{3s+2}|7s-1-0| + (2\times3)\sum_{k=1}^{s}|7s-2-1| + (3\times4)\sum_{k=1}^{s}|7s-4-3|$$
$$+(4\times2)\sum_{k=1}^{s-1}|7s-7k-(7k-1)|$$
$$= 4(3s+2)(7s-1) + 6s(7s-3) + 12s(7s-7) + 16(7s+1)\left\lfloor\frac{s}{2}\right\rfloor - 112\left(\left\lfloor\frac{s}{2}\right\rfloor^2 + \left\lfloor\frac{s}{2}\right\rfloor\right) - 16(7s+1)\left(s-1-\left\lfloor\frac{s}{2}\right\rfloor\right) + 112\left(s-1-\left\lfloor\frac{s}{2}\right\rfloor\right)\left(\left\lfloor\frac{s}{2}\right\rfloor + s\right)$$
$$= -224\left\lfloor\frac{s}{2}\right\rfloor^2 + 224s\left\lfloor\frac{s}{2}\right\rfloor - 192\left\lfloor\frac{s}{2}\right\rfloor + 210s^2 - 74s + 8. \quad \square$$

Corollary 2.2. *For poly-methyl methacrylate network $PMMA(s)$ with $s \geq 1$, we have*

1. $W^+Mo_t(PMMA(s)) = -336\lfloor\frac{s}{2}\rfloor^2 + 336s\lfloor\frac{s}{2}\rfloor - 288\lfloor\frac{s}{2}\rfloor + 378s^2 - 42s + 4.$
2. $W^*Mo_t(PMMA(s)) = -448\lfloor\frac{s}{2}\rfloor^2 + 448s\lfloor\frac{s}{2}\rfloor - 384\lfloor\frac{s}{2}\rfloor + 420s^2 - 148s + 16.$

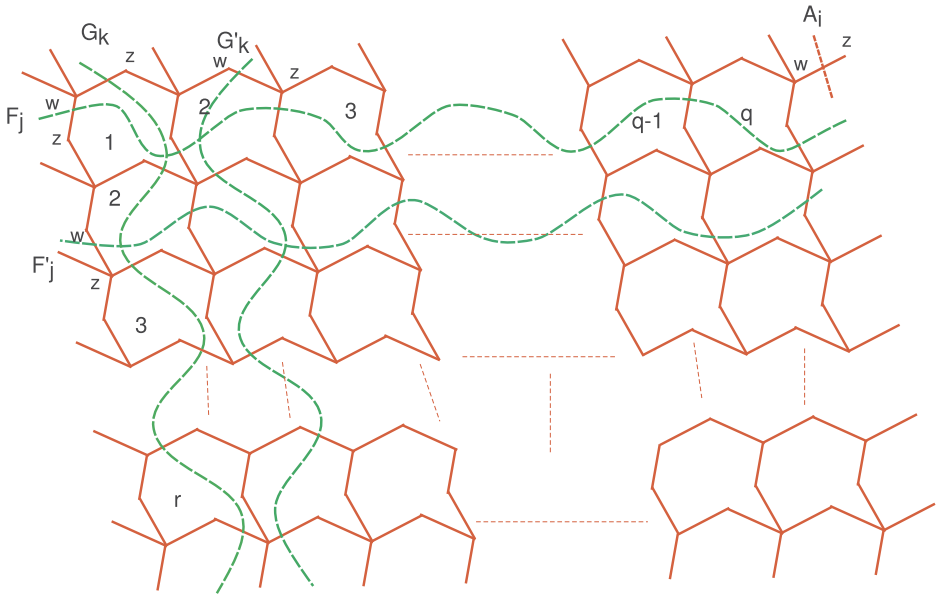

Fig. 3. Cuts of SIO_2 layer structure.

Table 5
The values of $n_{SIO_2}(w)$ and $n_{SIO_2}(z)$ with their respective degrees in A_i, F_j, F'_j, G_k and G'_k.

$wz \in E_{SIO_2}$	$n_{SIO_2}(w)$	$n_{SIO_2}(z)$	$deg_{SIO_2}(w)$	$deg_{SIO_2}(z)$	Frequency
A_i	$3qr+4(q+r+1)$	1	4	1	1
$F_j = F'_j$	$(3q+4)j+\left\lfloor\frac{q+1}{2}\right\rfloor$	$(3q+4)(r-j+1)+\left\lceil\frac{q+1}{2}\right\rceil$	4	2	$q+1$
$G_k = G'_k$	$(3r+4)k+\left\lfloor\frac{r+1}{2}\right\rfloor$	$(3r+4)(q-k+1)+\left\lceil\frac{r+1}{2}\right\rceil$	4	2	$r+1$

2.3. Weighted Mostar invariants of SIO_2 nanostructure

SIO_2 is a massive covalent composition of oxygen and silicon atoms. Silicon dioxide SIO_2 has two oxygen atoms for every silicon atom. The silicon dioxide molecular structure can be used to create an octagonal structure. When such octagons are linked next to each other, they form a SIO_2 layer structure, as demonstrated by Fig. 3. The layer structure of SIO_2 has order $|V(SIO_2)| = 3qr+4(q+r)+5$ and size $|E(SIO_2)| = 4(qr+q+r+1)$. We introduced three types of cuts in order to cover all the edges of SIO_2 layer structure. We define the pendant cuts of $SIO_2(\mathrm{q},\mathrm{r})$ as $\{Ai : 1 \le i \le 2(q+r+2)\}$, which lie on the boundary of its layer structure. Every pendent cuts individually covers a single edge in layer structure of SIO_2 and all of them are relatively symmetric. The horizontal cuts F_j and F'_j are symmetric to each other, where $1 \le j \le r$. Moreover the vertical cuts G_k and G'_k, where $1 \le k \le q$ are also relatively symmetric. In Table 5, we calculated the values of $n_{SIO_2}(w)$ and $n_{SIO_2}(z)$ with their respective degrees in A_i, F_j, F'_j, G_k and G'_k. Weighted vertex, edge and total Mostar invariants of SIO_2 nanostructure are evaluated next.

Theorem 2.5. *For $SIO_2(\mathrm{q},\mathrm{r})$ nanostructure with $(q,r \ge 1)$, we have*

1. $W^+Mo_v(SIO_2) = 10(q+r+2)(3qr+4q+4r+3)+24\lceil\frac{r}{2}\rceil(4+(3q+7)q)(r-\lceil\frac{r}{2}\rceil)+12(q+1)(2\lceil\frac{r}{2}\rceil-r)(\lceil\frac{q+1}{2}\rceil-\lfloor\frac{q+1}{2}\rfloor)+24\lceil\frac{q}{2}\rceil(4+(3r+7)r)(q-\lceil\frac{q}{2}\rceil)+12(r+1)(2\lceil\frac{q}{2}\rceil-q)(\lceil\frac{r+1}{2}\rceil-\lfloor\frac{r+1}{2}\rfloor)$.
2. $W^*Mo_v(SIO_2) = 8(q+r+2)(3qr+4q+4r+3)+32\lceil\frac{r}{2}\rceil(4+(3q+7)q)(r-\lceil\frac{r}{2}\rceil)+16(q+1)(2\lceil\frac{r}{2}\rceil-r)(\lceil\frac{q+1}{2}\rceil-\lfloor\frac{q+1}{2}\rfloor)+32\lceil\frac{q}{2}\rceil(4+(3r+7)r)(q-\lceil\frac{q}{2}\rceil)+16(r+1)(2\lceil\frac{q}{2}\rceil-q)(\lceil\frac{r+1}{2}\rceil-\lfloor\frac{r+1}{2}\rfloor)$.

Proof. First, we have the following results. Using the values of $n_{SIO_2}(w)$ and $n_{SIO_2}(z)$ with their specific degrees from Table 5, we obtain the following:

$$W^{+}Mo_{v}(SIO_2) = (4+1)\sum_{i=1}^{2(q+r+2)} |3qr+4(q+r+1)-(1)| + 2(4+2)(q+1)\sum_{j=1}^{r}\left|3qj+4j+\left\lfloor\frac{q+1}{2}\right\rfloor - \left(3q(r-j)+3q+4(r-j)+4+\left\lceil\frac{q+1}{2}\right\rceil\right)\right| + 2(4+2)(r+1)\sum_{k=1}^{q}\left|3rk+4k+\left\lfloor\frac{r+1}{2}\right\rfloor - \left(3r(q-k)+3r+4(q-k)+4+\left\lceil\frac{r+1}{2}\right\rceil\right)\right|$$

$$= (5)(2)(q+r+2)(3qr+4q+4r+3) + (2)(6)(q+1)\sum_{j=1}^{\lceil\frac{r}{2}\rceil}\left((3q+4)(r+1)+\left\lceil\frac{q+1}{2}\right\rceil - \left\lfloor\frac{q+1}{2}\right\rfloor - 2(3qj+4j)\right) + (2)(6)(q+1)\sum_{j=\lceil\frac{r}{2}\rceil}^{r}\left(2(3qj+4j)-(3q+4)(r+1)-\left\lceil\frac{q+1}{2}\right\rceil + \left\lfloor\frac{q+1}{2}\right\rfloor\right) + (2)(6)(r+1)\sum_{k=1}^{\lceil\frac{q}{2}\rceil}\left((3r+4)(q+1)+\left\lceil\frac{r+1}{2}\right\rceil - \left\lfloor\frac{r+1}{2}\right\rfloor - 2(3rk+4k)\right) + (2)(6)(r+1)\sum_{k=\lceil\frac{q}{2}\rceil}^{q}\left(2(3rk+4k)-(3r+4)(q+1)-\left\lceil\frac{r+1}{2}\right\rceil + \left\lfloor\frac{r+1}{2}\right\rfloor\right)$$

$$= 10(q+r+2)(3qr+4q+4r+3) + 24\left\lceil\frac{r}{2}\right\rceil(4+(3q+7)q)\left(r-\left\lceil\frac{r}{2}\right\rceil\right) + 12(q+1)\left(2\left\lceil\frac{r}{2}\right\rceil - r\right)\left(\left\lceil\frac{q+1}{2}\right\rceil - \left\lfloor\frac{q+1}{2}\right\rfloor\right) + 24\left\lceil\frac{q}{2}\right\rceil(4+(3r+7)r)\left(q-\left\lceil\frac{q}{2}\right\rceil\right) + 12(r+1)\left(2\left\lceil\frac{q}{2}\right\rceil - q\right)\left(\left\lceil\frac{r+1}{2}\right\rceil - \left\lfloor\frac{r+1}{2}\right\rfloor\right).$$

$$W^{*}Mo_{v}(SIO_2) = (4\times 1)\sum_{i=1}^{2(q+r+2)} |3qr+4(q+r+1)-(1)| + 2(4\times 2)(q+1)\sum_{j=1}^{r}\left|3qj+4j+\left\lfloor\frac{q+1}{2}\right\rfloor - \left(3q(r-j)+3q+4(r-j)+4+\left\lceil\frac{q+1}{2}\right\rceil\right)\right| + 2(4\times 2)(r+1)\sum_{k=1}^{q}\left|3rk+4k+\left\lfloor\frac{r+1}{2}\right\rfloor - \left(3r(q-k)+3r+4(q-k)+4+\left\lceil\frac{r+1}{2}\right\rceil\right)\right|$$

$$W^{*}Mo_{v}(SIO_2) = (4)(2)(q+r+2)(3qr+4q+4r+3) + (2)(8)(q+1)\sum_{j=1}^{\lceil\frac{r}{2}\rceil}\left((3q+4)(r+1)+\left\lceil\frac{q+1}{2}\right\rceil - \left\lfloor\frac{q+1}{2}\right\rfloor - 2(3qj+4j)\right) + (2)(8)(q+1)\sum_{j=\lceil\frac{r}{2}\rceil}^{r}\left(2(3qj+4j)-(3q+4)(r+1)-\left\lceil\frac{q+1}{2}\right\rceil + \left\lfloor\frac{q+1}{2}\right\rfloor\right) + (2)(8)(r+1)\sum_{k=1}^{\lceil\frac{q}{2}\rceil}\left((3r+4)(q+1)+\left\lceil\frac{r+1}{2}\right\rceil - \left\lfloor\frac{r+1}{2}\right\rfloor - 2(3rk+4k)\right) + (2)(8)(r+1)\sum_{k=\lceil\frac{q}{2}\rceil}^{q}\left(2(3rk+4k)-(3r+4)(q+1)-\left\lceil\frac{r+1}{2}\right\rceil + \left\lfloor\frac{r+1}{2}\right\rfloor\right)$$

$$= 8(q+r+2)(3qr+4q+4r+3) + 32\left\lceil\frac{r}{2}\right\rceil(4+(3q+7)q)\left(r-\left\lceil\frac{r}{2}\right\rceil\right) + 16(q+1)\left(2\left\lceil\frac{r}{2}\right\rceil - r\right)\left(\left\lceil\frac{q+1}{2}\right\rceil - \left\lfloor\frac{q+1}{2}\right\rfloor\right) + 32\left\lceil\frac{q}{2}\right\rceil(4+(3r+7)r)\left(q-\left\lceil\frac{q}{2}\right\rceil\right) + 16(r+1)\left(2\left\lceil\frac{q}{2}\right\rceil - q\right)\left(\left\lceil\frac{r+1}{2}\right\rceil - \left\lfloor\frac{r+1}{2}\right\rfloor\right). \quad \square$$

Theorem 2.6. *For $SIO_2(\mathrm{q},\mathrm{r})$ nanostructure with $(q, r \geq 1)$, we have*

1. $W^{+}Mo_{e}(SIO_2) = 10(q+r+2)(4qr+4q+4r+3) + 12(q+1)^2(2\lceil\frac{r}{2}\rceil(4r-4\lceil\frac{r}{2}\rceil-1)+r) + 24(q+1)\lceil\frac{q+1}{2}\rceil(2\lceil\frac{r}{2}\rceil-r) + 12(r+1)^2(2\lceil\frac{q}{2}\rceil(4q-4\lceil\frac{q}{2}\rceil-1)+q) + 24(r+1)\lceil\frac{r+1}{2}\rceil(2\lceil\frac{q}{2}\rceil-q)$.
2. $W^{*}Mo_{e}(SIO_2) = 8(q+r+2)(4qr+4q+4r+3) + 16(q+1)^2(2\lceil\frac{r}{2}\rceil(4r-4\lceil\frac{r}{2}\rceil-1)+r) + 32(q+1)\lceil\frac{q+1}{2}\rceil(2\lceil\frac{r}{2}\rceil-r) + 16(r+1)^2(2\lceil\frac{q}{2}\rceil(4q-4\lceil\frac{q}{2}\rceil-1)+q) + 32(r+1)\lceil\frac{r+1}{2}\rceil(2\lceil\frac{q}{2}\rceil-q)$.

Proof. Similarly to previous proof, we have the following results. Using the values of $m_{SIO_2}(w)$ and $m_{SIO_2}(z)$ with their respective

Table 6
The values of $m_{SIO_2}(w)$ and $m_{SIO_2}(z)$ with their respective degrees in A_i, F_j, F'_j, G_k and G'_k.

$wz \in E_{SIO_2}$	$m_{SIO_2}(w)$	$m_{SIO_2}(z)$	$deg_{SIO_2}(w)$	$deg_{SIO_2}(z)$	Frequency
A_i	$4(qr+q+r)+3$	0	4	1	1
$F_j = F'_j$	$4(q+1)j - \left\lceil \frac{q+1}{2} \right\rceil$	$(q+1)(4r+3-4j) + \left\lceil \frac{q+1}{2} \right\rceil$	4	2	$q+1$
$G_k = G'_k$	$4(r+1)k - \left\lceil \frac{r+1}{2} \right\rceil$	$(r+1)(4q+3-4k) + \left\lceil \frac{r+1}{2} \right\rceil$	4	2	$r+1$

degrees from Table 6, we have the following:

$$
\begin{aligned}
W^{+}Mo_e(SIO_2) &= (4+1)\sum_{i=1}^{2(q+r+2)} |4(qr+q+r)+3| + 2(4+2)(q+1)\sum_{j=1}^{r} |4(q+1)j - \left\lceil \frac{q+1}{2} \right\rceil - \\
&\left((q+1)(4r+3-4j) + \left\lceil \frac{q+1}{2} \right\rceil\right)| + 2(4+2)(r+1)\sum_{k=1}^{q} |4(r+1)k - \left\lceil \frac{r+1}{2} \right\rceil - \\
&\left((r+1)(4q+3-4k) + \left\lceil \frac{r+1}{2} \right\rceil\right)| \\
&= (5)(2)(q+r+2)(4qr+4q+4r+3) + (2)(6)(q+1)\sum_{j=1}^{\lceil \frac{r}{2} \rceil}((q+1)(4r+3)+2 \\
&\left\lceil \frac{q+1}{2} \right\rceil - 8(q+1)j\Big) + (2)(6)(q+1)\sum_{j=\lceil \frac{r}{2} \rceil}^{r}\left(8(q+1)j - (q+1)(4r+3) - 2\left\lceil \frac{q+1}{2} \right\rceil\right) \\
&+ (2)(6)(r+1)\sum_{j=1}^{\lceil \frac{q}{2} \rceil}\left((r+1)(4q+3) + 2\left\lceil \frac{r+1}{2} \right\rceil - 8(r+1)k\right) + (2)(6)(r+1)\sum_{j=\lceil \frac{q}{2} \rceil}^{q} \\
&\left(8(r+1)k - (r+1)(4q+3) - 2\left\lceil \frac{r+1}{2} \right\rceil\right). \\
&= 10(q+r+2)(4qr+4q+4r+3) + 12(q+1)^2\left(2\left\lceil \frac{r}{2} \right\rceil(4r - 4\left\lceil \frac{r}{2} \right\rceil - 1) + r\right) + 24 \\
&(q+1)\left\lceil \frac{q+1}{2} \right\rceil\left(2\left\lceil \frac{r}{2} \right\rceil - r\right) + 12(r+1)^2\left(2\left\lceil \frac{q}{2} \right\rceil(4q - 4\left\lceil \frac{q}{2} \right\rceil - 1) + q\right) + 24(r+1) \\
&\left\lceil \frac{r+1}{2} \right\rceil\left(2\left\lceil \frac{q}{2} \right\rceil - q\right). \\
W^{*}Mo_e(SIO_2) &= (4\times 1)\sum_{i=1}^{2(q+r+2)} |4(qr+q+r)+3| + 2(4\times 2)(q+1)\sum_{j=1}^{r} |4(q+1)j - \left\lceil \frac{q+1}{2} \right\rceil - \\
&\left((q+1)(4r+3-4j) + \left\lceil \frac{q+1}{2} \right\rceil\right)| + 2(4\times 2)(r+1)\sum_{k=1}^{q} |4(r+1)k - \left\lceil \frac{r+1}{2} \right\rceil - \\
&\left((r+1)(4q+3-4k) + \left\lceil \frac{r+1}{2} \right\rceil\right)| \\
&= (4)(2)(q+r+2)(4qr+4q+4r+3) + (2)(8)(q+1)\sum_{j=1}^{\lceil \frac{r}{2} \rceil}((q+1)(4r+3)+2 \\
&\left\lceil \frac{q+1}{2} \right\rceil - 8(q+1)j\Big) + (2)(8)(q+1)\sum_{j=\lceil \frac{r}{2} \rceil}^{r}\left(8(q+1)j - (q+1)(4r+3) - 2\left\lceil \frac{q+1}{2} \right\rceil\right) \\
&+ (2)(8)(r+1)\sum_{j=1}^{\lceil \frac{q}{2} \rceil}\left((r+1)(4q+3) + 2\left\lceil \frac{r+1}{2} \right\rceil - 8(r+1)k\right) + (2)(8)(r+1)\sum_{j=\lceil \frac{q}{2} \rceil}^{q} \\
&\left(8(r+1)k - (r+1)(4q+3) - 2\left\lceil \frac{r+1}{2} \right\rceil\right). \\
&= 8(q+r+2)(4qr+4q+4r+3) + 16(q+1)^2\left(2\left\lceil \frac{r}{2} \right\rceil(4r - 4\left\lceil \frac{r}{2} \right\rceil - 1) + r\right) + 32 \\
&(q+1)\left\lceil \frac{q+1}{2} \right\rceil\left(2\left\lceil \frac{r}{2} \right\rceil - r\right) + 16(r+1)^2\left(2\left\lceil \frac{q}{2} \right\rceil(4q - 4\left\lceil \frac{q}{2} \right\rceil - 1) + q\right) + 32(r+1) \\
&\left\lceil \frac{r+1}{2} \right\rceil\left(2\left\lceil \frac{q}{2} \right\rceil - q\right). \quad \square
\end{aligned}
$$

Corollary 2.3. *For $SIO_2(\mathrm{q},\mathrm{r})$ nanostructure with $(q, r \geq 1)$, we have*

1. $W^{+}Mo_t(SIO_2) = 10(q+r+2)(7qr+8q+8r+6)+24\lceil\frac{r}{2}\rceil(4+(3q+7)q)(r-\lceil\frac{r}{2}\rceil)+12(q+1)^2(2\lceil\frac{r}{2}\rceil(4r-4\lceil\frac{r}{2}\rceil-1)+r)+12(q+1)(2\lceil\frac{r}{2}\rceil-r)(3\lceil\frac{q+1}{2}\rceil-\lfloor\frac{q+1}{2}\rfloor)+24\lceil\frac{q}{2}\rceil(4+(3r+7)r)(q-\lceil\frac{q}{2}\rceil)+12(r+1)^2(2\lceil\frac{q}{2}\rceil(4q-4\lceil\frac{q}{2}\rceil-1)+q)+12(r+1)(2\lceil\frac{q}{2}\rceil-q)(3\lceil\frac{r+1}{2}\rceil-\lfloor\frac{r+1}{2}\rfloor)$.
2. $W^{*}Mo_t(SIO_2) = 8(q+r+2)(7qr+8q+8r+6)+32\lceil\frac{r}{2}\rceil(4+(3q+7)q)(r-\lceil\frac{r}{2}\rceil)+16(q+1)^2(2\lceil\frac{r}{2}\rceil(4r-4\lceil\frac{r}{2}\rceil-1)+r)+16(q+1)(2\lceil\frac{r}{2}\rceil-r)(3\lceil\frac{q+1}{2}\rceil-\lfloor\frac{q+1}{2}\rfloor)+32\lceil\frac{q}{2}\rceil(4+(3r+7)r)(q-\lceil\frac{q}{2}\rceil)+16(r+1)^2(2\lceil\frac{q}{2}\rceil(4q-4\lceil\frac{q}{2}\rceil-1)+q)+16(r+1)(2\lceil\frac{q}{2}\rceil-q)(3\lceil\frac{r+1}{2}\rceil-\lfloor\frac{r+1}{2}\rfloor)$.

3. Conclusion

This article explored how weighted Mostar invariant can be assessed for various nanostructures using cut method. All such indices have been affirmed to be deployed in QSAR/QSPR studies which are crucial for chemical hazard assessment, novel drug exploration, and molecular configuration. Using the cut method, we have obtained numerical expressions for the weighted Mostar invariants of molecular graphs of melem chains $MC(h)$ nanostructure, poly-methyl methacrylate network $PMMA(s)$ and silicon dioxide SIO_2 nanostructure. Our findings could be useful for the models of QSPR/QSAR correlation in order to discuss the properties of these molecular graphs.

Funding Statement

No Explicit funding has been received for this study.

Ethical approval

Not applicable.

CRediT authorship contribution statement

Zahid Raza: Resources, Investigation, Formal analysis, Conceptualization. **Noor ul Huda:** Writing – original draft, Visualization, Validation, Software, Methodology, Data curation. **Farhana Yasmeen:** Writing – review & editing, Writing – original draft, Visualization, Validation, Software, Methodology, Investigation, Data curation. **Kashif Ali:** Resources, Project administration, Funding acquisition, Formal analysis, Data curation, Conceptualization. **Shehnaz Akhter:** Writing – original draft, Software, Methodology, Investigation, Funding acquisition, Data curation, Conceptualization. **Yuqing Lin:** Writing – original draft, Software, Resources, Project administration, Methodology, Investigation, Funding acquisition.

Declaration of competing interest

The authors declare the following financial interests/personal relationships which may be considered as potential competing interests: Zahid Raza is the Associate Editor for Heliyon. If there are other authors, they declare that they have no known competing financial interests or personal relationships that could have appeared to influence the work reported in this paper.

Data availability

No additional data set is required to support the study.

Acknowledgements

Z.R. is partially supported by the University of Sharjah Research Grant No. 23021440148 and MASEP Research Group.

References

[1] M.O. Albertson, The irregularity of a graph, Ars Comb. 46 (1997) 219–225.
[2] M. Arockiaraj, J. Clement, N. Tratnik, Mostar indices of carbon nanostructures and circumscribed donut benzenoid systems, Int. J. Quant. Chem. 119 (24) (2019) e26043.
[3] S. Akhter, Z. Iqbal, A. Aslam, W. Gao, Computation of Mostar index for some graph operations, Int. J. Quant. Chem. 121 (15) (2021) e26674.
[4] S. Akhter, Two degree distance based topological indices of chemical trees, IEEE Access 7 (2019) 95653–95658.
[5] K. Balasubramanian, Integration of graph theory and quantum chemistry for structure-activity relationships, SAR QSAR Environ. Res. 2 (1–2) (1994) 59–77.
[6] A.T. Balaban, Topological and stereochemical molecular descriptors for databases useful in QSAR, similarity/dissimilarity and drug design, SAR QSAR Environ. Res. 8 (1–2) (1998) 1–21.
[7] S.A.U.H. Bokhary, M. Imran, S. Akhter, S. Manzoor, Molecular topological invariants of certain chemical networks, Main Group Met. Chem. 44 (1) (2021) 141–149.
[8] T. Došlić, B. Furtula, A. Graovac, I. Gutman, S. Moradi, Z. Yarahmadi, On vertex-degree-based molecular structure descriptors, MATCH Commun. Math. Comput. Chem. 66 (2011) 613–626.

[9] T. Došlić, T. Reti, D. Vukicevic, On the vertex degree indices of connected graphs, Chem. Phys. Lett. 512 (4–6) (2011) 283–286.
[10] D. Dimitrov, S. Brandt, H. Abdo, The total irregularity of a graph, Discrete Math. Theor. Comput. Sci. 16 (2014).
[11] T. Došlić, I. Martinjak, R. Škrekovski, R. Tipurić Spužević, I. Zubac, Mostar invariant, J. Math. Chem. 56 (10) (2018) 2995–3013.
[12] K. Deng, S. Li, Extremal catacondensed benzenoids with respect to the Mostar invariant, J. Math. Chem. 58 (7) (2020) 1437–1465.
[13] E. Estrada, The Structure of Complex Networks: Theory and Applications, Oxford University Press, Inc., New York, NY, USA, 2011.
[14] I. Gutman, Degree-based topological indices, Croat. Chem. Acta 86 (4) (2013) 351–361.
[15] W. Gao, Z. Iqbal, S. Akhter, M. Ishaq, A. Aslam, On irregularity descriptors of derived graphs, AIMS Math. 5 (5) (2020) 4085–4107.
[16] T.U. Islam, Z.S. Mufti, A. Ameen, M.N. Aslam, A. Tabraiz, On certain aspects of topological indices, J. Math. (2021).
[17] M. Imran, S. Akhter, Z. Iqbal, On the eccentric connectivity polynomial of-sum of connected graphs, Complexity (2020).
[18] M. Imran, S. Akhter, Z. Iqbal, Edge Mostar invariant of chemical structures and nanostructures using graph operations, Int. J. Quant. Chem. 120 (15) (2020) e26259.
[19] B. Jurgens, E. Irran, J. Senker, P. Kroll, H. Muller, W. Schnick, Melem (2, 5, 8-triamino-tri-s-triazine), an important intermediate during condensation of melamine rings to graphitic carbon nitride: synthesis, structure determination by X-ray powder diffractometry, solid-state NMR, and theoretical studies, J. Am. Chem. Soc. 125 (34) (2003) 10288–10300.
[20] D.C. Jagger, A. Harrison, K.D. Jandt, The reinforcement of dentures, J. Oral Rehabil. 26 (3) (1999) 185–194.
[21] Y.K. Kim, S. Grandini, J.M. Ames, L.S. Gu, S.K. Kim, D.H. Pashley, J.L. Gutmann, F.R. Tay, Critical review on methacrylate resin-based root canal sealers, J. Orthod. 36 (3) (2010) 383–399.
[22] S. Klavzar, I. Gutman, B. Mohar, Labeling of benzenoid systems which reflects the vertex-distance relations, J. Chem. Inf. Comput. Sci. 35 (3) (1995) 590–593.
[23] R. Natarajan, New topological indices with very high discriminatory power, SSAR QSAR Environ. Res. 22 (1–2) (2011) 1–20.
[24] R.V. Sole, S. Valverde, Information theory of complex networks: on evolution and architectural constraints, in: Complex Networks, Springer, Berlin, Heidelberg, 2004, pp. 189–207.
[25] N. Tratnik, Computing the Mostar invariant in networks with applications to molecular graphs, Iran. J. Math. Chem. 12 (1) (2021) 1–18.
[26] D. Vukičević, M. Gasperov, Bond additive modeling 1, Adriatic indices, Croat. Chem. Acta 83 (3) (2010) 243–260.
[27] D. Vukičević, Bond additive modeling 2. Mathematical properties of max-min rodeg invariant, Croat. Chem. Acta 83 (3) (2010) 261–273.
[28] D. Vukičević, Bond additive modeling 4, QSPR and QSAR studies of the variable Adriatic indices, Croat. Chem. Acta 84 (1) (2011) 87–91.
[29] Z. Raza, K. Naz, S. Ahmad, Expected values of molecular descriptors in random polyphenyl chains, Emerg. Sci. J. 6 (1) (2022) 151–165.
[30] H. Yang, M. Imran, S. Akhter, Z. Iqbal, M.K. Siddiqui, On distance-based topological descriptors of subdivision vertex-edge join of three graphs, IEEE Access 7 (2019) 143381–143391.